

Intranuclear Inclusions of Expanded Polyglutamine Protein in Spinocerebellar Ataxia Type 3

H. L. Paulson,^{*†#} M. K. Perez,<sup>* Y. Trottier,[§]
J. Q. Trojanowski,[‡] S. H. Subramony,^{||} S. S. Das,^{*}
P. Vig,^{||} J.-L. Mandel,[§] K. H. Fischbeck,[†]
and R. N. Pittman^{*}</sup>

^{*}Department of Pharmacology

[†]Department of Neurology

[‡]Department of Pathology

University of Pennsylvania School
of Medicine

Philadelphia, Pennsylvania 19104

[§]Institut de Genetique et de Biologie
Moleculaire et Cellulaire

67404 Illkirch Cedex

France

^{||}Department of Neurology

University of Mississippi

Jackson, Mississippi 38677

Summary

The mechanism of neurodegeneration in CAG/polyglutamine repeat expansion diseases is unknown but is thought to occur at the protein level. Here, in studies of spinocerebellar ataxia type 3, also known as Machado-Joseph disease (SCA3/MJD), we show that the disease protein ataxin-3 accumulates in ubiquitinated intranuclear inclusions selectively in neurons of affected brain regions. We further provide evidence *in vitro* for a model of disease in which an expanded polyglutamine-containing fragment recruits full-length protein into insoluble aggregates. Together with recent findings from transgenic models, our results suggest that intranuclear aggregation of the expanded protein is a unifying feature of CAG/polyglutamine diseases and may be initiated or catalyzed by a glutamine-containing fragment of the disease protein.

Introduction

A growing number of neurodegenerative diseases are now known to be caused by an expanded CAG trinucleotide repeat that encodes polyglutamine in the disease protein (Bates, 1996; Zoghbi, 1996; Paulson and Fischbeck, 1996). To date, the list includes Huntington's disease (HD), spinal and bulbar muscular atrophy, dentatorubral-pallidoluysian atrophy, and five dominantly inherited ataxias—spinocerebellar ataxia (SCA) types 1–3, 6, and 7 (La Spada et al., 1991; Huntington's Disease Collaborative Research Group, 1993; Orr et al., 1993; Kawaguchi et al., 1994; Koide et al., 1994; Nagafuchi et al., 1994; Imbert et al., 1996; Lindblad et al., 1996; Pulst et al., 1996; Sanpei et al., 1996; Zhuchenko et al., 1997). These disorders are thought to share a common pathogenesis occurring at the protein level. Expansion of the

glutamine repeat appears to confer upon the disease protein a toxic gain of function that is selectively deleterious to neurons (Housman, 1995; Ross, 1995; Bates, 1996; MacDonald and Gusella, 1996). Theoretical models and a growing body of experimental evidence suggest that expanded glutamine repeats may alter protein interactions, but precisely how this causes neurodegeneration is unknown (Perutz et al., 1994; Li et al., 1995; Stott et al., 1995; Bao et al., 1996; Burke et al., 1996; Ikeda et al., 1996; Kahlem et al., 1996; Kalchman et al., 1997; Wanker et al., 1997).

For several reasons, models attempting to explain the mechanism of neurodegeneration in this group of diseases are increasingly focussed on the glutamine repeat itself (Bates, 1996; Perutz, 1996). First, the disease proteins are entirely dissimilar outside of the polyglutamine tract. Second, disease severity increases with longer glutamine repeats in each disease (although the threshold repeat length for developing disease differs slightly for each disease). Third, and most important, several transgenic models employing protein fragments with an expanded glutamine repeat have yielded neurodegenerative phenotypes (Ikeda et al., 1996; Mangiarini et al., 1996). Experimental results from several laboratories are consistent with a model in which expanded polyglutamine adopts a "pathologic conformation" (Trottier et al., 1995b) and engages in inappropriate protein-protein interactions, perhaps even including aggregation of the disease protein (Ikeda et al., 1996).

Protein aggregation mediated by the expanded glutamine domain is a compelling model for the molecular basis of disease, in part because it is so common a theme in other neurodegenerative diseases. But whereas well defined pathologic structures support theories of aggregation in, for example, Alzheimer's disease, none of the CAG/polyglutamine diseases is known to have neuropathologic changes that support a model of aggregation. In addition, no adequate theory has yet explained why, in each CAG/polyglutamine disease, only selective brain regions are affected, despite widespread expression of the disease proteins.

As a model for the CAG/polyglutamine repeat diseases, we have chosen to study spinocerebellar ataxia type 3, also known as Machado-Joseph disease (SCA3/MJD; Rosenberg, 1992). This CAG/polyglutamine repeat disorder may be the most common dominantly inherited ataxia worldwide (Maciel et al., 1995; Maruyama et al., 1995; Matilla et al., 1995; Ranum et al., 1995; Schols et al., 1995; Durr et al., 1996). The clinical features of SCA3/MJD vary, but typically include ataxia together with bulbar, extrapyramidal, and pyramidal signs. The most frequent pathologic findings are degeneration within the deep basal ganglia, the brainstem, the spinal cord, and, to a lesser extent, the cerebellum (Sachdev et al., 1982; Yuasa et al., 1986; Takiyama et al., 1994). The disease gene *MJD1* encodes an intracellular protein of unknown function, ataxin-3, which with a predicted molecular weight of 42 kDa is the smallest of the polyglutamine disease proteins (Kawaguchi et al., 1994). The CAG/glutamine repeat lies near the carboxyl terminus, where

To whom correspondence should be addressed. Present address: Department of Neurology, University of Iowa Hospitals, Iowa City, IA 52242.

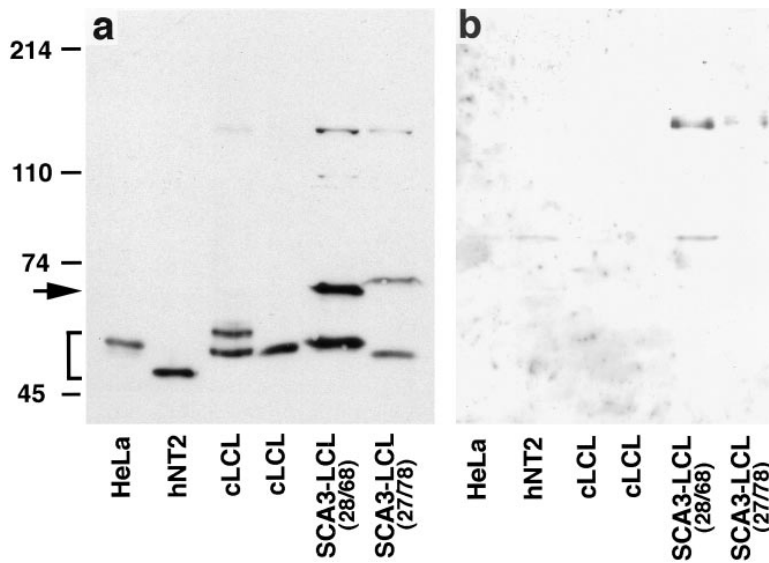


Figure 1. Western Blot for Ataxin-3
Ataxin-3 antiserum specifically recognizes normal and expanded repeat ataxin-3. Shown are results with human cell lines probed sequentially with immune (a) and preimmune (b) serum. The bracket indicates normal ataxin-3, which varies in size because of normal CAG repeat length polymorphism, and the arrow indicates expanded ataxin-3 in two SCA3/MJD lymphoblastoid cell lines (SCA3-LCL). Normal and expanded CAG repeat lengths are noted in parentheses for the SCA3/MJD LCLs. Abbreviations for cell lines are HeLa (HeLa cells), hNT2 (differentiated human N-Tera2 neurons), and cLCL (control lymphoblastoid lines).

it is normally 12–37 repeats and becomes expanded to 61–84 repeats in affected individuals.

In this paper, we present evidence for aberrant localization and probable aggregation of this polyglutamine disease protein in human disease tissue. Our studies of SCA3/MJD brain demonstrate that ataxin-3, normally a predominantly cytoplasmic protein, accumulates in ubiquitinated nuclear inclusions (NI) that are found selectively in neurons known to be affected by the disease process. The results take on an added significance in light of recent findings showing neuronal NI in transgenic models of other polyglutamine diseases (Davies et al., 1997; H. Orr and H. Zoghbi, personal communication) and suggest that, although the various polyglutamine disease proteins normally may be present in different cellular compartments, the nucleus is a primary site of pathogenesis for this class of diseases. In further studies in vitro, we present evidence supporting a model of disease in which full-length disease protein is recruited into aggregates by a polyglutamine fragment.

Results

Nuclear Inclusions (NI) of Ataxin-3 in Neurons of SCA3/MJD Brain

In an earlier study, we generated antiserum specific for the *MJD1* gene product ataxin-3 (Paulson et al., 1997). Figure 1 shows a representative immunoblot with this antiserum, also the principal immune serum used in the current study. With this antiserum, we previously demonstrated that both normal and expanded repeat ataxin-3 are expressed widely in diseased brain and throughout the body. In immunohistochemical studies of normal brain, ataxin-3 was localized to neuronal and nonneuronal cells in a predominantly, but not exclusively, cytoplasmic distribution. Staining also extended into neuronal processes and occasionally was observed within the nuclei of neurons in a faint punctate pattern.

In diseased brain, the subcellular distribution of ataxin-3 differs in at least one important respect: in several brain regions that are known targets of disease,

there is strong immunostaining for ataxin-3 within the nuclei of neurons (Figure 2). In individual neurons, this staining takes the form of one to three spherical intranuclear structures varying in size from 0.5 to ~6 μm in diameter. In some neurons, the inclusion spans more than half the diameter of the nucleus, but the most commonly observed pattern is a singlet or doublet structure near to, yet clearly distinct from, the hematoxylin-stained nucleolus (Figure 2d). NI were seen in both ethanol- and formaldehyde-fixed tissue, with short and long postmortem intervals. Staining was not observed with preadsorbed or preimmune serum or in the absence of primary serum. The inclusions were not autofluorescent, thus distinguishing them from the inclusions seen in the rare disorder, neuronal intranuclear inclusion disease (NIID; Palo et al., 1984; Garen et al., 1986; Weidenheim and Dickson, 1995).

NI were seen only in neurons and never in glial cells, despite the fact that many glial cells stain for ataxin-3 in normal and in diseased brain (Paulson et al., 1997). NI were found most frequently in neurons of the ventral pons, a primary target region in SCA3/MJD (Sachdev et al., 1982; Yuasa et al., 1986; Takiyama et al., 1994). They were also seen, less frequently, in other regions known to be affected in disease: substantia nigra, globus pallidus, dorsal medulla, and dentate nucleus. NI were not found in regions typically spared in disease, including cerebral cortex, hippocampus, striatum, and the Purkinje cell layer of the cerebellum. Even though it is generally not thought to be a major target in disease, the inferior olivary complex contained infrequent NI.

To confirm that these structures were specific to the disease state, we quantitated NI in the ventral pons of four SCA3/MJD brains and five control brains (Table 1). NI were present in all four SCA3/MJD brains, with one or more NI found in slightly less than half the neurons. NI were absent from all five controls. The frequency of NI in several other affected regions was lower but not quantitated.

To confirm that the inclusions contain ataxin-3, we performed double labeling immunofluorescence in

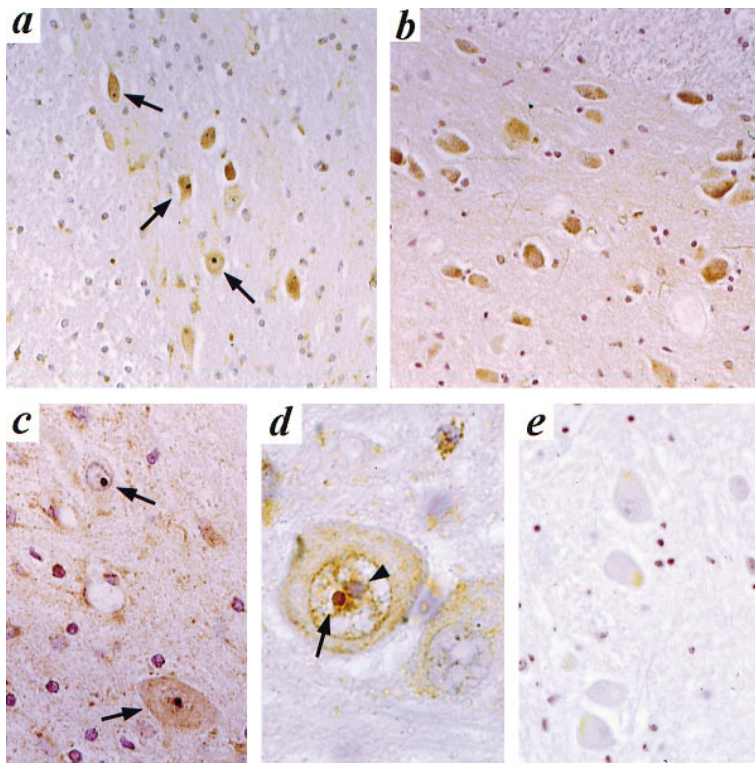


Figure 2. Nuclear Inclusions (NI) Containing Ataxin-3 in SCA3/MJD Brain

Ataxin-3 immunohistochemical staining in ventral pons from diseased brain ([a],[c], and [d]) demonstrates immunoreactive NI in neurons (arrows). At higher magnification, NI are distinct from, but often adjacent to, the hematoxylin-stained nucleolus (arrowhead in [d]). In control pons (b), NI were not seen, but note the normal predominantly cytoplasmic immunostaining for ataxin-3. Preadsorbed control is shown in (e). NI were also observed in other brain regions known be affected in disease (not shown). Magnifications before publication, 300× ([a] and [b]), 600× (c), 1500× (d), and 400× (e).

which the polyclonal ataxin-3 antiserum was paired with a monoclonal antibody (MAb) specific for ataxin-3 (1H9) or with MAb 1C2, the polyglutamine-specific antibody that preferentially recognizes expanded glutamine domains (Trottier et al., 1995b). In diseased brain, both MAbs labeled the same nuclear structures as did the polyclonal antiserum (Figure 3). Serial confocal images taken through an inclusion demonstrated the immunofluorescence signal in all focal planes, indicating that ataxin-3 is present throughout these structures (Figure 3). Staining of NI with 1C2 further confirms that the pathologic expanded glutamine domain is present within these inclusions.

Ataxin-3 Inclusions Are Ubiquitinated

Ubiquitination is a common feature of many neuropathologic structures, such as the Lewy body of Parkinson's disease (Lowe et al., 1993; Galvin et al., 1997). Its presence in neuropathologic structures is thought to reflect aberrant protein folding or degradation. We therefore determined whether NI also contain ubiquitin. In coimmunofluorescence studies, ubiquitin colocalized with

ataxin-3 throughout the inclusion (Figure 3). As with ataxin-3 immunostaining, ubiquitin immunostaining demonstrated that NI size varies considerably, in some cases nearly fully occupying the nucleus (Figure 4a; see also the lower portion of Figure 3). Again, brain regions that are known targets of disease showed intranuclear ubiquitin staining, whereas unaffected regions did not.

In a systematic survey of brain regions, ubiquitin-positive spherical bodies were found only in neurons and were nearly always intranuclear; only two clearly cytoplasmic ubiquitin inclusions were seen in two thoroughly examined SCA3/MJD brains. It is important to note, however, that ubiquitination in SCA3/MJD brain is not limited to NI. In affected regions, for example, densely immunoreactive deposits were often seen near neurons (Figure 4c). We do not know whether these represent the residue of dead or dying neurons or ubiquitin-positive nonneuronal cells; staining of adjacent thin sections with ataxin-3 antisera indicated that many of these deposits contain ataxin-3 (not shown). Diffuse cytoplasmic labeling for ubiquitin was also seen in some neurons of the substantia nigra and cervical cord. Lastly, many larger ubiquitin-positive structures resembling corpora amylacea were observed in the globus pallidus, pons, and medulla (not shown). However, since corpora amylacea are also seen as a normal feature of aging brain (Dickson et al., 1990), their relevance to the disease process is uncertain.

Many ubiquitin-positive pathologic structures contain antigenic determinants from cytoskeletal proteins or cytoskeletal-associated proteins. However, immunohistochemical staining with a panel of antibodies for such proteins was negative, suggesting that the NI of SCA3/MJD do not contain these proteins (Table 2). Particularly

Table 1. Quantitation of Ataxin-3 Nuclear Inclusions in SCA3/MJD Pons

Tissue	Neurons with Inclusions (% ± SD)
SCA3/MJD (N = 4) ^a	44.6% ± 17.9% ^c
Control (N = 5) ^b	0.0% ± 0.0%

^afrom three unrelated families with molecularly confirmed SCA3/MJD

^bthree controls without neurologic disease and two with Alzheimer's disease as irrelevant disease controls

^c~20% of positive neurons had more than one inclusion

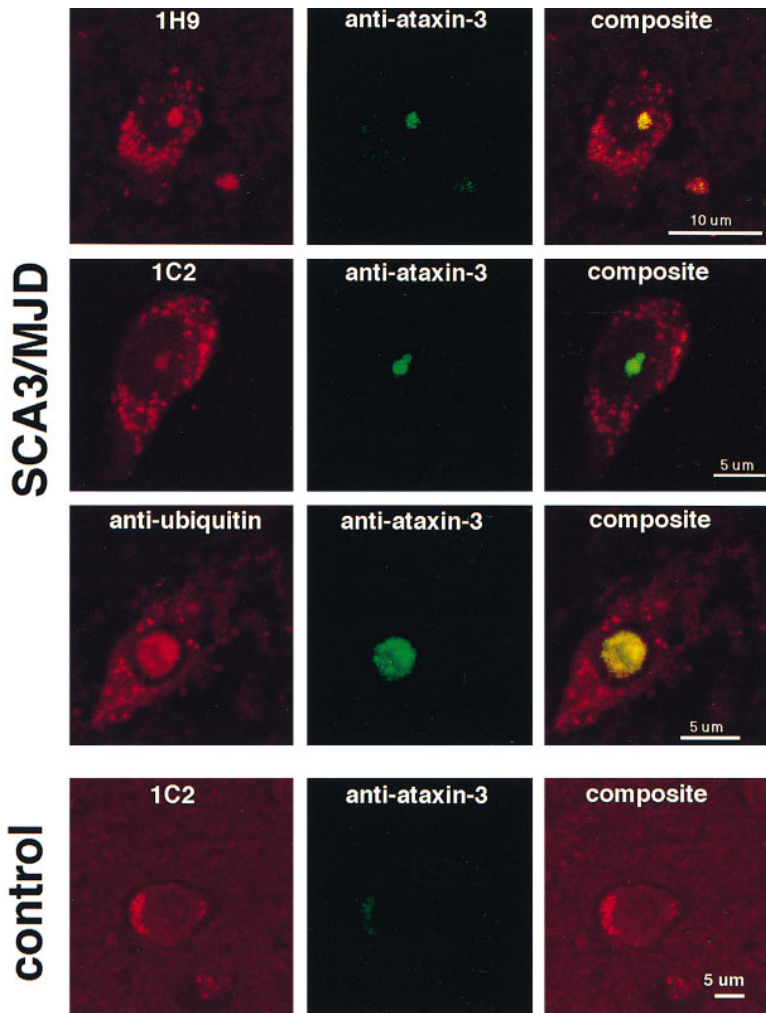


Figure 3. Coimmunofluorescence Analysis Confirming the Presence of Ataxin-3, Expanded Polyglutamine, and Ubiquitin within NI

Shown are confocal coimmunofluorescence images of SCA3/MJD pontine neurons (top three rows) and a control pontine neuron (bottom row) labeled with ataxin-3-specific MAb 1H9, polyglutamine-specific MAb 1C2, or anti-ubiquitin (left), together with ataxin-3 polyclonal antiserum (center). Composite images (right) demonstrate colocalization of label in NI in SCA3/MJD neurons; note that 1C2 weakly labels NI, yielding a green instead of a yellow composite image. The punctate cytoplasmic labeling seen in the rhodamine images is largely autofluorescence, is seen in both diseased and control neurons, and roughly defines the nuclear border. All sets of panels are summed images through the entire inclusion, except the anti-ubiquitin panels (third row from the top), which represent a single 0.5 μm focal plane through the center of a large inclusion, demonstrating that immunolabel is present deep within the structure.

notable is the absence of staining for neurofilament proteins, a common component of many ubiquitinated structures, including Lewy bodies and the inclusions of NIID (Palo et al., 1984; Lowe et al., 1993; Galvin et al., 1997).

Intracellular Aggregates Formed by an Expanded Glutamine Fragment

The presence in SCA3/MJD of NI containing ataxin-3 suggested that expanded ataxin-3 aggregates within the nucleus. To model this *in vitro*, we transfected human kidney epithelial 293T cells with expression constructs

encoding either full-length ataxin-3 or a carboxy-terminal fragment of the protein consisting of the glutamine repeat with short flanking sequences. For these studies, the normal and expanded polyglutamine tracts were 27 and 78 repeats, respectively. In transfected cells, we observed diffuse cytoplasmic staining for full-length ataxin-3 with a normal or expanded glutamine repeat, as well as for the truncated protein containing a normal repeat (Figure 5A). This result is consistent with our observation that endogenous ataxin-3 has a predominantly cytoplasmic distribution in several human cell lines (unpublished data).

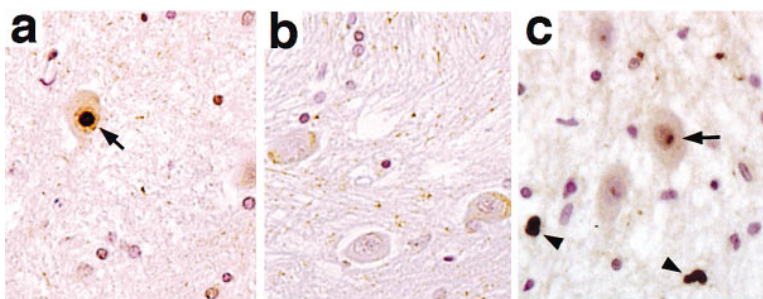


Figure 4. Ubiquitin Immunohistochemistry
NI in affected SCA3/MJD brain regions immunolabeled with anti-ubiquitin antiserum. Images show a diseased pons showing a single large intranuclear inclusion (arrow in [a]); a control pons labeled with anti-ubiquitin antiserum (b); and a diseased pons demonstrating ubiquitin-positive deposits that are seen in affected brain regions (arrowheads in [c]), often near neurons containing NI (arrows). Magnifications before publication, 400 \times ([a] and [b]) and 600 \times (c).

Table 2. Antibody Immunolabeling of Nuclear Inclusions

Antiserum	Antigen	Dilution	Inclusion Staining
anti-ataxin-3	ataxin-3 (polyclonal)	2,500	+++
1H9	ataxin-3 (mAb)	100	++
2B6	ataxin-3 (mAb)	100	–
1C2	TBP/polyGln	400	++
1C2	expanded polyGln	15,000	+
anti-ubiquitin	polyubiquitin	500	+++
anti-actin	actin	100	–
bTubulin	tubulin	1,000	–
MAP1B	MAP 5	500	–
AP14	MAP 2	neat	–
anti-NFL	NFL, Pind/tail	2,000	–
TA51	NFH, P+/tail within MPR	neat	–
RmdO9	NFH, P–/tail within MPR	neat	–
RM024	NFH P+++ /tail within MPR	10	–
PHF-6	paired helical filament	5,000	–
anti-vimentin	vimentin	100	–
anti-peripherin	peripherin	100	–
anti-desmin	desmin	neat	–
AE3	keratin	100	–
AE1	keratin	neat	–
GA5	GFAP	500	–

Abbreviations: TBP, TATA-binding protein; MAP, microtubule associated protein; NFL and NFH, neurofilament light and heavy chains; P+++ , heavily phosphorylated epitope; P+ , lightly phosphorylated epitope; P- , non- or poorly phosphorylated epitope; Pind, phosphorylation-independent epitope; MPR, multiphosphorylation repeat; GFAP, glial fibrillary acidic protein.

In contrast, truncated protein with an expanded repeat did not distribute diffusely within the cytoplasm but rather localized to two distinct subcellular structures: large cytoplasmic (and occasionally nuclear) spherical bodies that resemble vacuoles under phase contrast optics and smaller intranuclear and perinuclear clusters (Figure 5A). Greater than 97% of cells transfected with the expanded polyglutamine fragment displayed the larger spherical structures, and many cells displayed both structures. The larger structures concentrated the lysosomal marker LysoTracker DND-99 and thus may represent acidotropic vesicles, possibly lysosomal in origin (data not shown). The smaller ataxin-3 inclusions did not appear vesicular, and were most intensely immunolabeled by the polyglutamine-specific MAb 1C2. Confocal imaging confirmed that these smaller clusters were localized to the intranuclear and perinuclear space (Figure 5B). Although they are smaller than the NI seen in diseased brain, their presence indicates that truncated ataxin-3 can be transported to the nucleus, where it may form microaggregates.

Others have shown that expression of an expanded glutamine fragment of ataxin-3 is cytotoxic to COS cells (Ikeda et al., 1996). Similarly, we find that truncated ataxin-3 with an expanded glutamine repeat induces cell death in 293T cells (Figure 5C). The cytotoxicity we observe, however, is less marked than that previously reported, even though the truncated ataxin-3 construct and repeat length used by us is similar. In our hands, for example, many transfected cells survive several days and continue to express the cotransfected marker gene *lacZ*.

Recruitment of Ataxin-3 into Aggregates

When expressed in transfected cells, truncated ataxin-3 with an expanded repeat forms insoluble high molecular weight complexes that electrophorese on SDS gels at

the top of the stack and separating gels (Figure 6A). Truncated ataxin-3 with a normal repeat does not form such complexes, although it may form SDS-resistant dimers. Likewise, full-length protein with a normal or expanded repeat does not form high molecular weight complexes. However, when coexpressed with an expanded glutamine fragment, full-length ataxin-3 is recruited into insoluble complexes (Figure 6B). This was determined by showing, in coexpression experiments, that the high molecular weight complexes now become recognizable by antibodies to epitopes present only in the full-length, but not the truncated, protein (results with the ataxin-3 specific MAb 2B6 are shown; ataxin-3 antiserum gave similar results in separate experiments). Significantly, recruitment of the full-length ataxin-3 into aggregates occurred to an appreciable extent only when an expanded glutamine repeat was present in the full protein (Figure 6B). These results suggest that a pathologic (expanded) glutamine fragment can serve to initiate or catalyze aggregation of the full-length protein. Moreover, the probability that this will occur is dependent upon the length of the glutamine repeat within the full protein.

Next, we determined whether, along with electrophoretic evidence for recruitment, there were corresponding changes in the cellular distribution of full-length ataxin-3. To do this, we expressed full-length ataxin-3 together with truncated protein containing an expanded repeat, and then performed coimmunofluorescence with antibodies that distinguished the two (Figure 7). In one set of experiments, MAb 2B6 and anti-hemagglutinin (HA) antibody were used to distinguish full length ataxin-3 from a tagged truncated protein, and in a second set of experiments, the two proteins were separately epitope tagged and distinguished with anti-myc and anti-HA antibodies. When coexpressed with the truncated protein, full-length ataxin-3 no longer

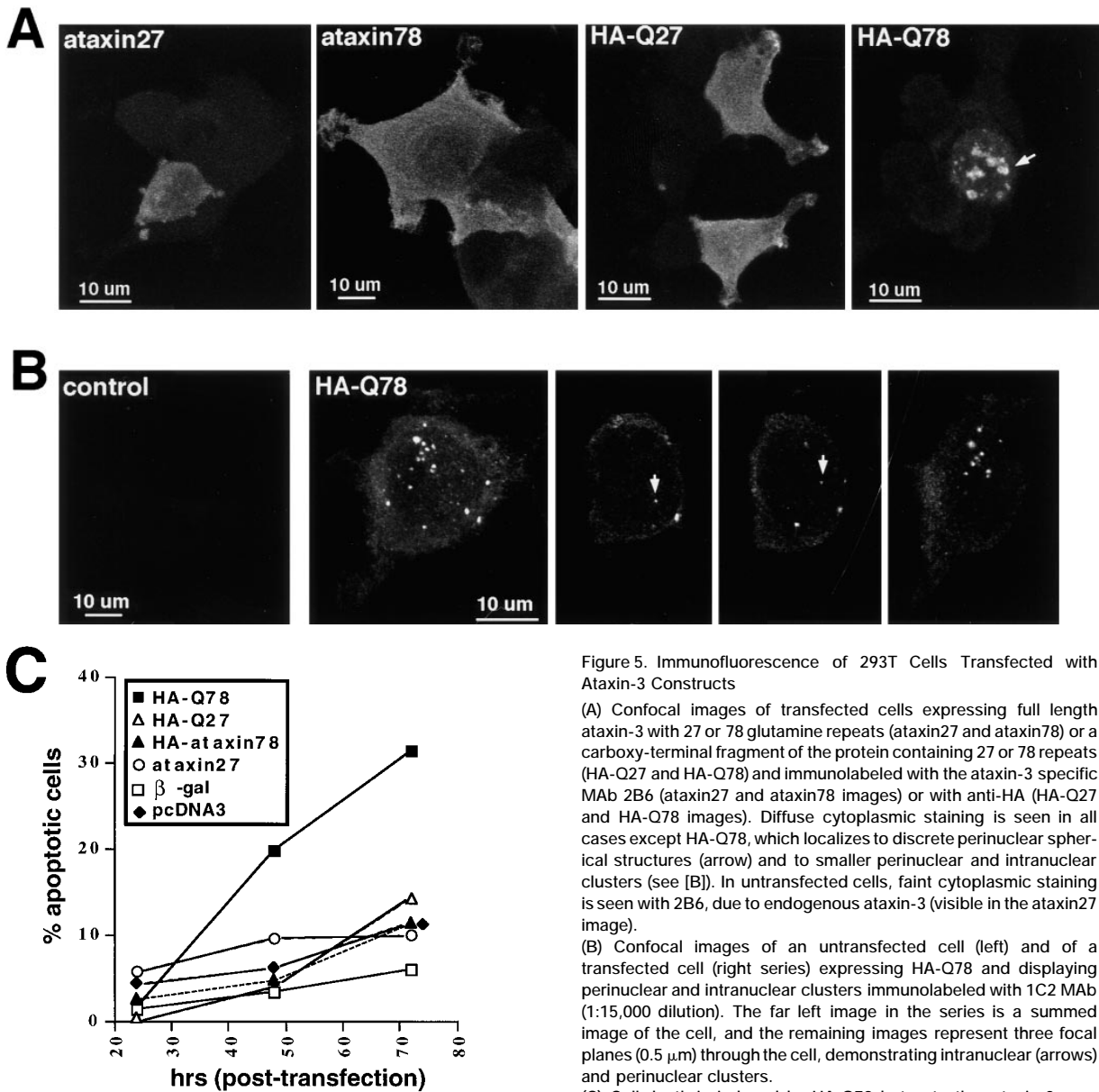


Figure 5. Immunofluorescence of 293T Cells Transfected with Ataxin-3 Constructs

(A) Confocal images of transfected cells expressing full length ataxin-3 with 27 or 78 glutamine repeats (ataxin27 and ataxin78) or a carboxy-terminal fragment of the protein containing 27 or 78 repeats (HA-Q27 and HA-Q78) and immunolabeled with the ataxin-3 specific MA b 2B6 (ataxin27 and ataxin78 images) or with anti-HA (HA-Q27 and HA-Q78 images). Diffuse cytoplasmic staining is seen in all cases except HA-Q78, which localizes to discrete perinuclear spherical structures (arrow) and to smaller perinuclear and intranuclear clusters (see [B]). In untransfected cells, faint cytoplasmic staining is seen with 2B6, due to endogenous ataxin-3 (visible in the ataxin27 image).

(B) Confocal images of an untransfected cell (left) and of a transfected cell (right series) expressing HA-Q78 and displaying perinuclear and intranuclear clusters immunolabeled with 1C2 MA b (1:15,000 dilution). The far left image in the series is a summed image of the cell, and the remaining images represent three focal planes (0.5 μ m) through the cell, demonstrating intranuclear (arrows) and perinuclear clusters.

(C) Cell death is induced by HA-Q78 but not other ataxin-3 constructs (inset). Results represent quantitation from 10 randomly selected fields for each construct. Results are representative of three experiments.

distributed diffusely in the cytoplasm. Instead, it colocalized with truncated protein to the same large spherical perinuclear structures that are formed in cells expressing just the truncated protein. In contrast to the gel electrophoresis results, which showed that only expanded repeat ataxin-3 tends to be recruited into insoluble complexes, the coimmunofluorescence studies demonstrate that both normal and expanded repeat ataxin-3 are recruited to the spherical structures by a coexpressed expanded glutamine fragment. Quantitation of colocalization showed that normal ataxin-3 essentially always colocalized with HA-Q78 to intracellular spherical structures (in one experiment, 97 out of 97 cells in randomly selected fields), and similar results

were obtained with expanded ataxin-3. In control experiments, neither of two irrelevant proteins, β -galactosidase and calbindin, colocalized to the subcellular ataxin-3 structures (Figure 7; data not shown). The results are consistent with a model in which recruitment is mediated through the glutamine domain of the full-length protein and occurs even with a glutamine repeat of normal length.

Together, the immunofluorescence and gel electrophoresis studies demonstrate that a coexpressed expanded glutamine fragment markedly alters the intracellular behavior of full-length ataxin-3. In at least one important respect, the changes induced by the glutamine fragment differ for normal and expanded ataxin-3.

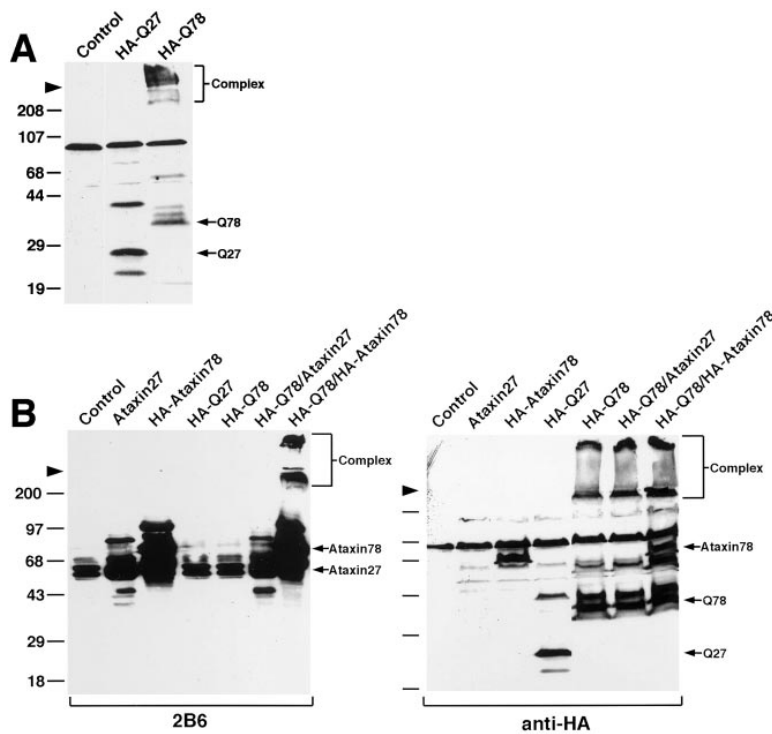


Figure 6. Recruitment of Expanded Ataxin-3 into Insoluble Aggregates

(A) Western blot of lysates from cells transfected with HA-Q27 or HA-Q78 alone. HA-Q78 forms insoluble complexes that migrate in the stack and at the top of the separating gel (arrowhead), while the normal glutamine repeat HA-Q27 forms little if any insoluble complex. Arrows indicate probable monomeric forms of Q27 and Q78. Both also generate higher molecular weight bands that may be SDS-resistant dimers.

(B) Full-length expanded ataxin-3 is recruited into insoluble complexes by coexpressed HA-Q78. Lysates from transfected cells were run in parallel on separate gels and probed with: (left) 2B6, which recognizes full-length ataxin-3 but not HA-Q27 or HA-Q78; and (right) anti-HA antibody, which recognizes HA-Q27, HA-Q78, and HA-ataxin78, but not untagged ataxin27. Whereas expanded repeat ataxin-3 is recruited into insoluble complexes (left panel, far right lane), normal repeat ataxin-3 is not (adjacent lane). Note that endogenous ataxin-3 in 293T cells is recognized by MAb 2B6. Results are representative of three experiments.

Whereas both normal and expanded ataxin-3 are recruited by an expanded glutamine fragment into subcellular structures, only expanded ataxin-3 is recruited into insoluble aggregates. The simplest interpretation is that the intermolecular bonds formed between two glutamine domains differ significantly, depending upon whether both domains are expanded versus only one of the two.

Discussion

While the genetic basis of the CAG/polyglutamine repeat diseases is clear, the molecular mechanism of neuronal degeneration remains uncertain. Our results from SCA3/MJD tissue argue strongly for a protein-mediated effect as the basis of disease. In particular, the presence of ubiquitinated NI containing ataxin-3 suggests that aggregation of the disease protein occurs within neurons. Although ataxin-3 is normally expressed widely in the CNS, there is a direct correlation between brain regions that display NI and regions that are known targets in disease, implying that neuronal NI are an integral part of the disease process. Together with recent evidence showing similar NI in transgenic models of other CAG/polyglutamine repeat diseases, our results suggest that the nucleus is a primary site of pathogenesis in this class of neurodegenerative disorders.

The Nucleus as a Primary Site of Pathogenesis

Are NI pathologic features shared by all CAG/polyglutamine diseases? Recent studies of two other diseases suggest that this may be the case. In the SCA1 transgenic mouse (Burrigh et al., 1995), degenerating Purkinje cells develop NI that contain the SCA1 gene

product, ataxin-1 (H. Orr and H. Zoghbi, personal communication). Moreover, in transfected cells, expanded ataxin-1 forms large intranuclear structures (H. Orr and H. Zoghbi, personal communication). In an HD transgenic mouse, neuronal NI are formed by a truncated huntingtin protein containing an expanded repeat (Davies et al., 1997). Because the transgene in this mouse model is only a single exon of the HD gene encoding a small amino-terminal polyglutamine fragment of the protein (Mangiarini et al., 1996), some might argue that it does not precisely mirror the human disease. However, similar intranuclear inclusions have already been noted in an earlier ultrastructural analysis of HD brain (Roizin et al., 1979). The presence of NI in three separate CAG/polyglutamine diseases or models of disease indicates that the disease process may be centered in the nucleus.

The distribution of NI in SCA3/MJD brain corresponds to regions that are known to be affected in disease. Despite this clear and direct correlation, we cannot assume a causal link between the presence of NI and neurodegeneration. Still, there are several plausible ways NI might perturb neuronal function. It is increasingly clear that nuclear events are exquisitely regulated in a spatial and temporal manner. On mechanical grounds alone, NI could disrupt spatially coordinated nuclear processes such as transcription and splicing. Alternatively, NI might sequester important nuclear factors, thereby altering gene expression. Because of its own polymorphic glutamine repeat (Imbert et al., 1994), the TATA-binding protein is one potential candidate for sequestration along with a polyglutamine disease protein. A third possibility is that the formation of NI reflects, or causes, a breakdown in normal proteolytic processes within the nucleus. Proteosomes are abundant in the nuclei of neurons (Mengual et al., 1996), suggesting that

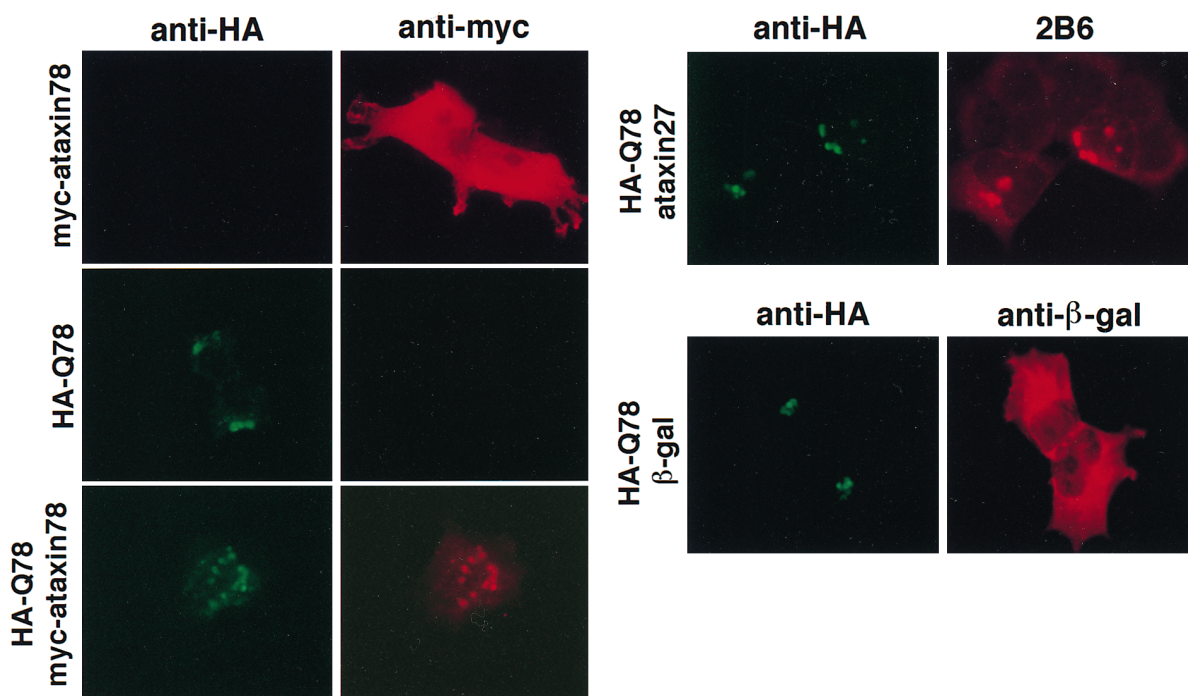


Figure 7. Cellular Redistribution of Ataxin-3 by Coexpressed HA-Q78

Paired coimmunofluorescence images of cells transfected with the indicated constructs (left) and immunolabeled with antibodies (top) separately detecting HA-Q78 (anti-HA antibody) and the cotransfected protein. Both normal and expanded ataxin-3 normally distribute diffusely in the cytoplasm but become localized to perinuclear structures when coexpressed with HA-Q78. The cellular distribution of two transfected control proteins, β -galactosidase (shown at right) and calbindin (not shown), is not altered by coexpression of HA-Q78. Shown are representative fields in all cases.

intracellular proteolysis is one way for the cell to precisely regulate the relative abundance of nuclear factors. Even subtle changes in normal nuclear proteolysis might perturb this homeostasis. Further molecular analysis of NI in SCA3/MJD should help determine whether nuclear functions are disrupted.

NI apparently form in CAG/polyglutamine repeat diseases regardless of the normal cellular distribution of the protein. While ataxin-1 is normally found in the nucleus, both huntingtin and ataxin-3 are predominantly cytoplasmic proteins (DiFiglia et al., 1995; Gutekunst et al., 1995; Servadio et al., 1995; Sharp et al., 1995; Trotter et al., 1995a; Paulson et al., 1997). In fact, further immunocytochemical studies of ataxin-3 in cell lines indicate that the protein's subcellular distribution is actually complicated and includes nuclear expression in a small percentage of cells (M. Perez and H. Paulson, unpublished data); and according to one report, huntingtin may localize to the nucleus as well as the cytoplasm (DeRoos et al., 1996). These facts raise an important question: do NI derive from a normal nuclear pool of the disease protein or from the larger cytoplasmic pool? Equally important, does the disease protein within NI represent the full protein, a polyglutamine fragment, or some combination? In CAG/polyglutamine diseases, the formation of polyglutamine-containing proteolytic fragments of the disease protein has been proposed as the mechanism of neurodegeneration (Goldberg et al., 1996; Ikeda et al., 1996). Although we have been unable to detect proteolytic fragments of ataxin-3 in diseased brain (Paulson et al., 1997), it is possible that they exist

in an inaccessible, insoluble form within NI. In SCA3/MJD, NI must contain regions of the ataxin-3 protein outside of the glutamine domain, because NI are labeled by 1H9, an ataxin-3 specific MAb that fails to recognize the carboxy-terminal glutamine fragment of the protein. Whether NI include the full protein, however, is unknown.

NI have been described in relatively few neurologic disorders, including viral diseases, oculopharyngeal muscular dystrophy (Blumen et al., 1996), and NIID (Palo et al., 1984; Garen et al., 1986; Weidenheim and Dickson, 1995). Clinically, the last of these most closely resembles CAG/polyglutamine diseases. Some patients with NIID develop progressive ataxia with extrapyramidal features, also one of the most common clinical presentations in several CAG/polyglutamine diseases. The two can, however, be distinguished on several grounds. NIID, which is a rare and probably heterogeneous disorder, does not show the dominant inheritance pattern of most CAG/polyglutamine diseases. Moreover, the inclusions in NIID, unlike those in SCA3/MJD, are autofluorescent, may contain neurofilament antigen, and are found throughout the brain. Still, some cases of adult onset NIID could represent sporadic forms of CAG/polyglutamine repeat diseases, a testable hypothesis now that antibodies are available for expanded polyglutamine tracts and many of the disease proteins.

Ubiquitination in Disease

NI of ataxin-3 are disease-specific structures, and as such constitute a pathologic hallmark of SCA3/MJD. The presence of ubiquitin, as well, in NI indicates that

they likely represent pathologic aggregates of the disease protein. Although ubiquitination is a normal part of the cell's proteolytic pathways, its occurrence in pathologic structures is thought to reflect misfolding, aggregation, or aberrant degradation of proteins (Lowe et al., 1993; Galvin et al., 1997). Except for a single report showing ubiquitination of huntingtin (Kalchman et al., 1996), very little is known about the normal degradation of polyglutamine disease proteins. It will be important to determine whether ataxin-3 normally is degraded via the ubiquitin-proteasome pathway, and whether this pathway is disrupted or altered by an expanded glutamine domain. Currently, it is unknown whether the ubiquitin within NI is covalently attached to ataxin-3 or to other proteins. Further biochemical analysis of ataxin-3 inclusions should help determine whether the disease protein is directly ubiquitinated and whether components of the proteasome are sequestered within these structures.

In SCA3/MJD, both the ubiquitin-positive NI and the presumably extracellular ubiquitin deposits are found only in affected brain regions, indicating that ubiquitination is either an integral part of, or at the very least a direct consequence of, the disease process. Our results, together with results showing ubiquitin in the NI of HD transgenic mice (Davies et al., 1997), imply that ubiquitination may be a general feature of CAG/polyglutamine diseases. It will be important to determine whether ubiquitination is seen in pathologic material from other CAG/polyglutamine diseases. Unfortunately, human disease tissue provides us with only a single glimpse in time of the last stage in the disease process. Based on our current studies of disease tissue, for example, we cannot know whether the ubiquitin deposits seen in the parenchyma of SCA3/MJD represent the end result of neurodegeneration. Careful and systematic analysis of transgenic models of disease will help determine the temporal relation of ubiquitination to cell death.

If ubiquitinated NI contain aggregated ataxin-3, why don't we observe high molecular weight complexes of ataxin-3 on electrophoretic analysis of disease tissue? We suspect that NI from diseased brain remain insoluble with standard techniques of homogenization, lysis, and sample preparation, and thus are too large to enter the stack of an SDS-polyacrylamide gel. If we succeed in developing denaturation procedures that can dissociate the insoluble complexes formed *in vitro*, the same denaturation procedures will be applied to homogenates from disease brain. It is possible, however, that the aggregates formed *in vitro* and *in vivo* are covalently linked by transglutaminase-mediated crosslinking (Green, 1993; Kahlem et al., 1996), in which case dissociation may be impossible.

Aggregation and Its Relationship to Cell Specificity

Because of our *in vivo* studies showing NI of ataxin-3, we sought to develop an *in vitro* model of polyglutamine-mediated aggregation. While no *in vitro* model can fully replicate a disease process occurring over decades, our results provide insight into possible mechanisms of aggregation in the disease state. In transfected cells, we have shown that a pathologic (expanded) glutamine fragment can (1) form intranuclear and perinuclear complexes, (2) cause a cellular redistribution of normal or

expanded ataxin-3, and (3) recruit expanded ataxin-3 into insoluble complexes. The last of these three depends upon the presence of an expanded repeat in the full protein, implying that recruitment into aggregates occurs via direct interactions between glutamine domains. Subcellular redistribution of full-length ataxin-3 also may be mediated directly through the glutamine domain, since control proteins lacking polyglutamine do not undergo cellular redistribution. We conclude that, *in vitro*, a pathologic polyglutamine fragment can serve as the seed or catalyst for glutamine-mediated aggregation of the full protein. If similar events take place *in vivo*, the CAG/polyglutamine repeat diseases may prove analogous to prion diseases, in which protease-resistant forms of prion can induce misfolding and/or aggregation of the normal prion protein (Come et al., 1993; DeArmond and Prusiner, 1995).

An intriguing feature of CAG/polyglutamine diseases is their cell specificity. Each disease causes degeneration only of neurons, and only in selective brain regions, despite widespread expression of the disease protein. Although higher expression levels of the disease protein in susceptible populations of neurons may contribute to this cell specificity, as has been reported in HD (Kosinski et al., 1997), this can only be part of the answer. Our results suggest that a pathogenic element in SCA3/MJD is the intranuclear aggregation of ataxin-3 in susceptible neurons. Based on our *in vivo* and *in vitro* studies, we propose that cell specificity is in part determined by differing propensities for ataxin-3 aggregation in different neuronal populations. In a subset of neurons, aggregation would be promoted by any of the following: (1) increased production of a proteolytic glutamine fragment; (2) increased misfolding of the nascent polypeptide or unfolding of the mature protein; (3) increased targeting of ataxin-3, or a proteolytic fragment, to the nucleus; and (4) increased total expression of ataxin-3. The last of these not only would raise local concentrations of the disease protein (perhaps thereby promoting self-aggregation), but in the process might lead to an increase in pathways (1) through (3) as well.

A widely held view is that cell specificity in CAG/polyglutamine repeat diseases arises, in part, from differences among neurons in the set of proteins that normally interact with the disease protein. This view and our proposed aggregation model are not mutually exclusive. On the contrary, normal interacting proteins might be expected to influence the disease protein's subcellular distribution, rate of degradation, probability of misfolding, and, most important, the degree to which its glutamine domain is exposed or sequestered. Any or all of these events could, in turn, influence the rate of aggregation.

Experimental Procedures

Pathologic Tissue

A total of six SCA3/MJD brains were examined, two cases each from three unrelated families (in all of whom expansion of the *MJD1* triplet repeat has been confirmed). The five control brains included three individuals without a history of neurologic illness and two individuals with a history of Alzheimer's disease as irrelevant disease controls. The shortest postmortem interval for an SCA3/MJD brain was <1 hr, and the longest was 22 hr; these two brains showed a similar frequency of NI.

Immunohistochemistry and Immunofluorescence

The antibodies and dilutions used in this study are shown in Table 2. Ataxin-3 polyclonal antiserum has been described (Paulson et al., 1997). MAbs 1H9 and 2B6 specifically bind ataxin-3 at regions amino-terminal to the glutamine tract and will be described in detail in a separate publication (Trottier et al., unpublished data). Epitope tag antibodies used in this study were the anti-hemagglutinin (HA) antibodies 12CA5 (Boehringer Mannheim) and Y11 (generously provided by D. Merry, Philadelphia) and the anti-myc antibody 9E10 (Calbiochem).

For immunohistochemistry of brain sections, 6 μm sections of paraffin-embedded tissue were processed and stained using the peroxidase-DAB technique as previously described (Paulson et al., 1997). Sections were typically counterstained with hematoxylin. In control experiments, the ataxin-3 polyclonal antiserum, anti-ubiquitin antiserum, and MAbs 1H9 and 1C2 were screened against sections of normal pons to ensure that the recognized NI were specific for disease tissue. All four antibodies specifically stained NI both by immunofluorescence and by immunohistochemistry. All other antibodies shown in Table 2 were screened against appropriate control brain sections, to verify that the specific antigen was detected at the concentration used.

For coimmunofluorescence studies of brain tissue, sections were labeled with primary antisera, followed by fluorescein isothiocyanate (FITC) goat anti-rabbit and rhodamine-goat anti-mouse sera, and viewed under standard epifluorescence with an XL-70 Minolta microscope or with a Leika LSBM laser confocal system coupled to a Leitz microscope. In confocal studies, we verified that no signal was obtained through the rhodamine channel after excitation for FITC, thus ensuring that signal crossover did not occur. FITC and rhodamine channels were collected simultaneously, and the digitized images were pseudocolored and recombined using Adobe Photoshop. For standard immunofluorescence, photographic slides were taken, scanned into digitized images, and processed with Adobe Photoshop.

MAB 1C2 recognizes expanded polyglutamine in ataxin-3 and other polyglutamine disease proteins (Trottier et al., 1995b) but also recognizes the glutamine repeat of TATA-binding protein, the protein against which it was initially raised (Lescure et al., 1994). However, at very low concentrations of the antiserum, 1C2 specifically binds to expanded glutamine tracts (I. An and E. Hirsch, personal communication). Therefore, in some immunohistochemistry experiments of brain tissue, and in all immunofluorescence studies of transfected cells, a 1:15,000 dilution of 1C2 was used. Immunohistochemical staining of NI was still present (albeit weaker) even at this lower concentration, confirming that the pathological expanded glutamine epitope of ataxin-3 exists within NI. For coimmunofluorescence experiments of human tissue, a 1C2 dilution of 1:400 was used.

Quantitation of NI

Four SCA3/MJD cases were chosen for analysis, based on the availability of equivalent sections through ventral mid-pons. Thin paraffin sections of ventral pons from four SCA3/MJD individuals (three separate families) and five controls were labeled immunohistochemically with affinity-purified ataxin-3 antiserum and scored for NI by an observer educated in the appearance of inclusions but blinded to the origin of the sections. In randomly selected sweeps at 400 \times , all pontine neurons in which the nucleus clearly was seen in cross section were scored for the presence or absence of immunohistochemically stained intranuclear spherical bodies. (To be seen and scored as a distinct structure, the diameter of an inclusion must be $\sim 0.5 \mu\text{m}$ or greater.) Neurons (110–150) were scored in each brain, and the percentage of neurons containing inclusions was determined for each sample. A mean percent value was then calculated, shown in Table 1.

In one SCA3/MJD brain (the case described by Paulson et al., 1997), we quantitated inclusions from adjacent regions of ventral pons that had been fixed separately with 70% ethanol/saline or 4% paraformaldehyde. Essentially identical results were obtained for both fixatives, confirming that the number of NI is independent of the method of fixation.

Expression Constructs and Transfection

For most transfections, we used the expression vector pCDNA3 containing either full-length or truncated ataxin-3. Constructs encoding full-length ataxin-3 with 27 or 78 CAG repeats, pCDNA3-MJD27 and pCDNA-HAMJD78, were previously described (Paulson et al., 1997); the latter has an HA epitope at the amino terminus of the protein. Truncated ataxin-3 constructs were generated by digesting ataxin-3 cDNA at the *Xmn*I site, 39 bp upstream of the CAG repeat, and placing the resultant carboxy-terminal ataxin-3 fragment into the *Sma*I site of the HA-tagging vector pJ3H (ATCC). The resulting truncated ataxin-3 protein consists of an amino-terminal HA epitope, 12 amino acids of ataxin-3 upstream of the glutamine repeat, the glutamine repeat (27 or 78 repeats), and the 43 amino acids comprising the carboxy-terminus of the protein. This HA-tagged construct was then subcloned into pCDNA3 for transfection studies (pCDNA-HAQ27 and pCDNA-HAQ78). Myc-tagged full-length ataxin-3 with 78 repeats was generated by subcloning ataxin-3 cDNA from pCDNA-HAMJD78 into the BamHI site of pJ3M (ATCC), thus replacing the HA epitope with a myc epitope at the amino terminus.

Subconfluent 293T cells were transfected using calcium phosphate precipitation (Sambrook et al., 1989). Twenty-four hours after transfection, cells were plated onto cover slips; 12 hr later, they were processed for immunofluorescence. Cells were fixed with 4% paraformaldehyde, permeabilized with 0.05% Triton X-100, and incubated in a blocking solution (2% normal goat serum in PBS with 0.05% Triton X-100) prior to incubations with antibody.

In some experiments, transfected cells were labeled with the organelle-specific dyes LysoTracker red DND-99 (50 nM) and Mitotracker green FM (200 nM; Molecular Probes) for 60 min prior to fixation. In these experiments, fixed cells were extracted with ice cold acetone, as recommended by the manufacturer, prior to subsequent immunofluorescence.

Cell Viability

In three similar experiments, 35 mm plates of cells were cotransfected with 2 μg total plasmid DNA in a 1:4 ratio of RSV- β Gal to one of the following: pCDNA-MJD78, pCDNA-MJD27, pCDNA-HAQ27, pCDNA-HAQ78, or pCDNA3 control plasmid. Viability was assessed by changes in the morphology of β -galactosidase-positive cells. At 48 and 72 hr after transfection, cells were washed in PBS, fixed in 4% paraformaldehyde and stained with X-Gal. Blue cells were scored as apoptotic or healthy (i.e., nonapoptotic), based on morphological criteria: small, round blebbing cells were scored as apoptotic and all other cells as healthy. For each sample, ten random fields were scored in a blinded manner. Cells transfected with HA-Q78 consistently showed an approximately threefold increase in apoptotic appearing cells when compared to all other transfected ataxin-3 constructs (see Figure 5C).

Quantitation of In Vitro Complexes

In cotransfection experiments, ten randomly selected fields of immunofluorescently labeled cells were viewed under FITC filter and scored for the total number of transfected cells expressing HA-Q78 or HA-Q27 and then for the number of positive cells in which staining was punctate (close to 100% for HA-Q78 and 0% for HA-Q27). The same fields were then viewed with the rhodamine filter, allowing us to determine the percent of ataxin27- or ataxin78-expressing cells (stained with anti-myc or 2B6) that showed precise colocalization to spherical structures. Quantitation was performed in a similar manner for cells transfected singly with ataxin27, ataxin78, HA-Q27, and HA-Q78, and for control cotransfections with HA-Q78 and calbindin or β -galactosidase. On average, ~ 100 cells were counted per experimental sample.

Gel Electrophoresis and Western Blot Analysis

Transfected cells were solubilized and prepared for SDS-polyacrylamide gel electrophoresis as described (Paulson et al., 1997). Equal volumes of equivalent lysates were electrophoresed on discontinuous 10% polyacrylamide gels, and both the separating and stacking portions of the gel were transblotted to polyvinylidene difluoride (PVDF) membrane (DuPont, New England Nuclear). Blots were incubated with affinity-purified ataxin-3 antiserum (1:1000), MAb 2B6 (1:1000) or anti-HA MAb 12CA5 (1:3000) in 5% nonfat milk/PBS, followed by horseradish peroxidase-conjugated goat anti-rabbit

(1:1000) or goat anti-mouse (1:10,000) antiserum. In some experiments (e.g., Figure 6), identical protein samples were run on separate gels and immunoblotted with separate antibodies in parallel. In others, blots were stripped and reprobed with a second antibody; stripping involved incubating blots 20 min at 45°C in 62.5 mM Tris-HCl (pH 6.8), 2% SDS, and 100 mM β -mercaptoethanol, followed by extensive washing in PBS. Immunoreactive bands were visualized by chemiluminescence (Renaissance, Du Pont-NEN).

Acknowledgements

We are grateful to the SCA3/MJD patients and their families for making this study possible through their generous donation of diseased tissue. We are indebted to M. Luise Schmidt for expert technical assistance with the confocal analyses and to A. Lee for help in making the HA-Q27 and HA-Q78 constructs. We thank Y. Lutz for assistance in production of the ataxin-3 specific MABs and J. Eberwine for generously allowing us to use his fluorescence microscope. For providing antibodies, we thank L. Tora (1C2), D. Merry (Y11), and J. Fields (9E10). This work was supported by grants from the Howard Hughes Medical Institute (H. P.), the American Academy of Neurology (H. L. P.), and the National Institutes of Health (R. P., K. F., and J. T.).

Received July 18, 1997; revised July 31, 1997.

References

Bates, G. (1996). Expanded glutamines and neurodegeneration—a gain of insight. *Bioessays* 18, 175–178.

Bao, J., Sharp, A.H., Wagster, M.V., Becher, M., Schilling, G., Ross, C.A., Dawson, V.L., and Dawson, T.M. (1996). Expansion of polyglutamine repeat in huntingtin leads to abnormal protein interactions involving calmodulin. *Proc. Natl. Acad. Sci. USA* 93, 5037–5042.

Blumen, S.C., Sadeh, M., Korczyn, A.D., Rouche, A., Nisipeanu, P., Asherov, A., and Tome, F.M. (1996). Intranuclear inclusions in oculopharyngeal muscular dystrophy among Bukhara Jews. *Neurology* 46, 1324–1328.

Burke, J.R., Enghild, J.J., Martin, M.E., You, Y.-S., Myers, R.M., Roses, A.D., Vance, J.M., and Strittmatter, W.J. (1996). Huntingtin and DRPLA proteins selectively interact with the enzyme GAPDH. *Nature Med.* 2, 347–350.

Burright, E.N., Clark, H.B., Servadio, A., Matilla, T., Feddersen, R.M., Yunis, W.S., Duvick, L.A., Zoghbi, H.Y., and Orr, H.T. (1995). SCA1 transgenic mice: a model for neurodegeneration caused by an expanded CAG repeat. *Cell* 82, 937–948.

Come, J.H., Fraser, P.E., and Lansbury, P.T., Jr. (1993). A kinetic model for amyloid formation in the prion diseases: importance of seeding. *Proc. Natl. Acad. Sci. USA* 90, 5959–5963.

Davies, S.W., Turmaine, M., Cozens, B.A., DiFiglia, M., Sharp, A.H., Ross, C.A., Scherzinger, E., Wanker, E.E., Mangiarini, L., and Bates, G.P. (1997). Formation of neuronal intranuclear inclusions underlies the neurological dysfunction in mice transgenic for the HD mutation. *Cell* 90, 537–548.

DeArmond, S.J., and Prusiner, S.B. (1995). Etiology and pathogenesis of prion diseases. *Am. J. Pathol.* 146, 785–811.

DeRoos, K.E., Dorsman, J.C., Smoor, M.A., Dunnen, J.T.D., and Ommen, G.-J.B.V. (1996). Subcellular localization of the Huntington's disease gene product in cell lines by immunofluorescence and biochemical subcellular fractionation. *Hum. Mol. Genet.* 5, 1093–1099.

Dickson, D.W., Wertkin, A., Kress, Y., Ksiuzak-Reding, H., and Yen, S.-H. (1990). Ubiquitin immunoreactive structures in normal human brains. *Lab. Invest.* 63, 87–99.

DiFiglia, M., Sapp, E., Chase, K., Schwarz, C., Meloni, A., Young, C., Martin, E., Vonsattel, J.-P., Carraway, R., Reeves, S.A., et al. (1995). Huntingtin is a cytoplasmic protein associated with vesicles in human and rat brain neurons. *Neuron* 14, 1075–1081.

Durr, A., Stevanin, G., Cancel, G., Duyckaerts, C., Abbas, N., Didier-jean, O., Chneiweiss, H., Benomar, A., Lyon-Caen, O., Julien, J., et

al. (1996). Spinocerebellar ataxia 3 and Machado-Joseph disease: clinical, molecular and neuropathologic features. *Ann. Neurol.* 39, 490–499.

Galvin, J.E., Lee, V.M.-Y., Schmidt, M.L., Tu, P.-H., Iwatsubo, T., and Trojanowski, J.Q. (1997). Pathobiology of the Lewy body (LB); studies of purified LBs, monoclonal antibodies and LB-like inclusions in transgenic animal models. *Adv. Neurol.*, in press.

Garen, P.D., Powers, J.M., Young, G.F., and Lee, V. (1986). Neuronal intranuclear hyaline inclusion disease in a nine year old. *Acta. Neuropathol.* 70, 327–332.

Goldberg, Y.P., Nicholson, D.W., Rasper, D.M., Kalchman, M.A., Koide, H.B., Graham, R.K., Bromm, M., Kazemi-Esfarjani, P., Thornberry, N.A., Vaillancourt, J.P., and Hayden, M.R. (1996). Cleavage of huntingtin by apopain, a proapoptotic cysteine protease, is modulated by the polyglutamine tract. *Nature Genet.* 13, 442–449.

Green, H. (1993). Human genetic diseases due to codon reiteration: relationship to an evolutionary mechanism. *Cell* 74, 955–956.

Gutekunst, C.-A., Levey, A.I., Heilman, C.J., Whaley, W.L., Yi, H., Nash, N.R., Rees, H.D., Madden, J.J., and Hersch, S.M. (1995). Identification and localization of huntingtin in brain and human lymphoblastoid cell lines with anti-fusion protein antibodies. *Proc. Natl. Acad. Sci. USA* 92, 8710–8714.

Housman, D. (1995). Gain of glutamines, gain of function? *Nature Genet.* 10, 3–4.

Huntington's Disease Collaborative Research Group (1993). A novel gene containing a trinucleotide repeat that is expanded and unstable on Huntington's disease chromosomes. *Cell* 72, 971–983.

Ikeda, H., Yamaguchi, M., Sugai, S., Aze, Y., Narumiya, S., Kakizuka, A. (1996). Expanded polyglutamine in the Machado-Joseph disease protein induces cell death in vitro and in vivo. *Nature Genet.* 13, 196–202.

Imbert, G., Trottier, Y., Beckmann, J., and Mandel, J.L. (1994). The gene for the TATA binding protein (TBP) that contains a highly polymorphic protein coding CAG repeat maps to 6q27. *Genomics* 21, 667–668.

Imbert, G., Saudou, F., Yvert, G., Devys, D., Trottier, Y., Garnier, J.-M., Weber, C., Mandel, J.-L., Cancel, G., Abbas, N., et al. (1996). Cloning of the gene for spinocerebellar ataxia 2 reveals a locus with high sensitivity to expanded CAG/glutamine repeats. *Nature Genet.* 14, 285–291.

Kahlem, P., Terre, C., Green, H., and Djian, P. (1996). Peptides containing glutamine repeats as substrates for transglutaminase-catalyzed crosslinking: relevance to diseases of the nervous system. *Proc. Natl. Acad. Sci. USA* 93, 14580–14585.

Kalchman, M.A., Graham, R.K., Xia, G., Koide, H.B., Hodgson, J.G., Graham, K.C., Goldberg, Y.P., Gietz, R.D., Pickart, C.M., Hayden, M.R. (1996). Huntingtin is ubiquitinated and interacts with a specific ubiquitin-conjugating enzyme. *J. Biol. Chem.* 271, 19385–19394.

Kalchman, M.A., Xia, G., Koide, H.B., McCutcheon, K., Graham, R.K., Nichol, K., Nishiyama, K., Kazemi-Esfarjani, P., Lynn, F.C., Wellington, C., et al. (1997). *HIP1*, a human homologue of *S. cerevisiae Sla2p*, interacts with membrane-associated huntingtin in the brain. *Nature Genet.* 16, 44–53.

Kawaguchi, Y., Okamoto, T., Taniwaki, M., Aizawa, M., Inoue, M., Katayama, H., Nakamura, S., Nishimura, M., Akiguchi, I., Kimura, J., Narumiya, S., and Kakizuka, A. (1994). CAG expansions in a novel gene for Machado-Joseph disease at chromosome 14q32.1. *Nature Genet.* 8, 221–228.

Koide, R., Ikeuchi, I., Onodera, O., Tanaka, H., Igarishi, S., Endo, K., Takahashi, H., Kondo, R., Ishikawa, A., Hayashi, T., et al. (1994). Unstable expansion of CAG repeat in hereditary dentatorubral-pallidolusian atrophy. *Nature Genet.* 6, 9–13.

Kosinski, C.M., Cha, J.-H., Young, A.B., Persichetti, F., MacDonald, M., Gusella, J.F., Penney, J.B., and Standaert, D.G. (1997). Huntingtin immunoreactivity in the rat neostriatum: differential accumulation in projection and interneurons. *Exp. Neurol.*, in press.

La Spada, A.R., Wilson, E.M., Lubahn, D.B., Harding, A.E., and Fischbeck, K.H. (1991). Androgen receptor gene mutations in X-linked spinal and bulbar muscular atrophy. *Nature* 352, 77–79.

Lescure, A., Lutz, Y., Eberhard, D., Jacq, X., Krol, A., Grummt, I.,

- Davidson, I., Chambon, P., and Tora, L. (1994). The N-terminal domain of the human TATA-binding protein plays a role in transcription from TATA-containing RNA polymerase II and III promoters. *EMBO J.* **13**, 1166–1175.
- Li, X.-J., Li, S.-H., Sharp, A.H., Nucifora, F.C., Jr, Schilling, G., Lanhahan, A., Worley, P., Snyder, S.H., and Ross, C.A. (1995). A huntingtin-associated protein enriched in brain with implications for pathology. *Nature* **378**, 398–402.
- Lindblad, K., Savontaus, M.-L., Stevanin, G., Holmberg, M., Digre, K., Zander, C., Ehrsson, H., David, G., Benomar, A., Nikoskelainen, E., Trotter, Y., Holmgren, G., Ptacek, L.J., Anttinen, A., Brice, A., and Schalling, M. (1996). An expanded CAG repeat sequence in spinocerebellar ataxia type 7. *Genome Res.* **6**, 965–971.
- Lowe, J., Mayer, R.J., and Landon, M. (1993). Ubiquitin in neurodegenerative diseases. *Brain Pathol.* **3**, 55–65.
- MacDonald, M.E., and Gusella, J.E. (1996). Huntington's disease: translating a CAG repeat into a pathogenic mechanism. *Curr. Opin. Neurobiol.* **6**, 638–643.
- Maciel, P., Gaspar, C., DeStefano, A.L., Silveira, I., Coutinho, P., Radvany, J., Dawson, D.M., Sudarsky, L., Guimares, J., Loureiro, J.E.L., et al. (1995). Correlation between CAG repeat length and clinical features in Machado-Joseph disease. *Am. J. Hum. Genet.* **57**, 54–61.
- Mangiarini, L., Sathasivam, K., Seller, M., Cozens, B., Harper, A., Heterington, C., Lawton, M., Trotter, Y., Lehrach, H., Davies, S.W., and Bates, G.P. (1996). Exon 1 of the HD gene with an expanded CAG repeat is sufficient to cause a progressive neurological phenotype in transgenic mice. *Cell* **87**, 493–506.
- Maruyama, H., Nakamura, S., Matsuyama, Z., Sakai, T., Doyu, M., Sobue, G., Seto, M., Tsujihata, M., Oh-i, T., Nishio, T., et al. (1995). Molecular features of the CAG repeats and clinical manifestation of Machado-Joseph disease. *Hum. Mol. Genet.* **5**, 807–812.
- Matilla, T., McCall, A., Subramony, S.H., and Zoghbi, H.Y. (1995). Molecular and clinical correlations in spinocerebellar ataxia type 3 and Machado-Joseph disease. *Ann. Neurol.* **38**, 68–72.
- Mengual, E., Arizti, P., Rodrigo, J., Gimenez-Amaya, J.M., and Castano, J.G. (1996). Immunohistochemical distribution and electron microscopic subcellular localization of the proteasome in the rat CNS. *J. Neurosci.* **16**, 6331–6341.
- Nagafuchi, S., Yanagisawa, H., Sato, K., Shirayama, T., Ohsaki, E., Bundo, M., Takeda, T., Tadakoro, K., Kondo, I., Murayama, N., et al. (1994). Dentatorubral and pallidoluysian atrophy expansion of an unstable CAG trinucleotide on chromosome 12p. *Nature Genet.* **6**, 14–18.
- Orr, H.T., Chung, M., Banfi, S., Kwiatkowski, T.J., Servadio, A., Beaudet, A.L., McCall, A.E., Duvick, L.A., Ranum, L.P.W., and Zoghbi, H.Y. (1993). Expansion of an unstable trinucleotide CAG repeat in spinocerebellar ataxia type 1. *Nature Genet.* **4**, 221–226.
- Palo, J., Haltia, M., Carpenter, S., Karpati, G., and Mushynski, W. (1984). Neurofilament subunit-related proteins in neuronal intranuclear inclusions. *Ann. Neurol.* **15**, 322–328.
- Paulson, H.L., and Fischbeck, K.H. (1996). Trinucleotide repeats in neurogenetic disorders. *Annu. Rev. Neurosci.* **19**, 79–107.
- Paulson, H.L., Das, S.S., Crino, P.B., Perez, M.K., Patel, S.C., Gotsdiner, D., Fischbeck, K.H., and Pittman, R.N. (1997). Machado-Joseph disease gene product is a cytoplasmic protein expressed widely in brain. *Ann. Neurol.* **41**, 453–462.
- Perutz, M.F. (1996). Glutamine repeats and inherited neurodegenerative diseases: molecular aspects. *Curr. Opin. Struct. Biol.* **6**, 848–858.
- Perutz, M.F., Johnson, T., Suzuki, M., and Finch, J.T. (1994). Glutamine repeats as polar zippers: their possible role in inherited neurodegenerative diseases. *Proc. Natl. Acad. Sci. USA* **91**, 5355–5358.
- Pulst, S.-M., Nechiporuk, A., Nechiporuk, T., Gispert, S., Chen, X.-N., Lopes-Cendes, I., Pearlman, S., Starkman, S., Orozco-Diaz, G., Lunke, A., et al. (1996). Moderate expansion of a normally biallelic trinucleotide repeat in spinocerebellar ataxia type 2. *Nature Genet.* **14**, 269–276.
- Ranum, L.P.W., Lundgren, J.K., Schut, L.J., Ahrens, M.J., Perlman, S., Aita, J., Bird, T.D., Gomez, C., and Orr, H.T. (1995). Spinocerebellar ataxia type I and Machado-Joseph disease: incidence of CAG expansions among adult-onset ataxia patients from 311 families with dominant, recessive or sporadic ataxia. *Am. J. Hum. Genet.* **57**, 603–608.
- Roizin, L., Stellar, S., and Liu, J.C. (1979). Neuronal nuclear-cytoplasmic changes in Huntington's chorea: electron microscope investigations. *Adv. Neurol.* **23**, 95–122.
- Rosenberg, R.N. (1992). Machado-Joseph disease: an autosomal dominant motor system degeneration. *Mov. Disord.* **7**, 193–203.
- Ross, C.A. (1995). When more is less: pathogenesis of glutamine repeat neurodegenerative diseases. *Neuron* **15**, 493–496.
- Sachdev, H.S., Forno, L.S., and Kane, C.A. (1982). Joseph disease: a multisystem degenerative disorder of the nervous system. *Neurology* **32**, 192–195.
- Sambrook, J., Fritsch, E.F., and Maniatis, T., eds. (1989). *Molecular Cloning: a Laboratory Manual* (Cold Spring Harbor, NY: Cold Spring Harbor Laboratory Press).
- Sanpei, K., Takano, H., Igarashi, S., Sato, T., Oyake, M., Sasaki, H., Wakisaka, A., Tashiro, K., Ishida, Y., Ikeuchi, T., et al. (1996). Identification of the spinocerebellar ataxia type 2 gene using a direct identification of repeat expansion and cloning technique, DIRECT. *Nature Genet.* **14**, 277–284.
- Schols, L., Vieri-Saecker, A.M.M., Schols, S., Przuntek, H., Epplen, J.T., and Riess, O. (1995). Trinucleotide expansion within the MJD1 gene presents clinically as spinocerebellar ataxia and occurs most frequently in German SCA patients. *Hum. Mol. Genet.* **4**, 1001–1005.
- Servadio, A., Koshy, B., Armstrong, D., Antalffy, B., Orr, H.T., and Zoghbi, H.Y. (1995). Expression analysis of the ataxin-1 protein in tissues from normal and spinocerebellar ataxia type 1 individuals. *Nature Genet.* **10**, 94–98.
- Sharp, A.H., Loev, S.J., Schilling, G., Li, S.-H., Li, X.-J., Bao, J., Wagster, M.V., Kotzuk, J.A., Steiner, J.P., Lo, A., et al. (1995). Widespread expression of Huntington's disease gene (IT15) protein product. *Neuron* **14**, 1065–1074.
- Stott, K., Blackburn, J.M., Butler, P.J.G., and Perutz, M. (1995). Incorporation of glutamine repeats makes protein oligomerize: implications for neurodegenerative diseases. *Proc. Natl. Acad. Sci. USA* **92**, 6509–6513.
- Takiyama, Y., Oyanagi, S., Kawashima, S., Sakamoto, H., Saito, K., Yoshida, M., Tsuji, S., Mizuno, Y., and Nishizawa, M. (1994). A clinical and pathologic study of a large Japanese family with Machado-Joseph disease tightly linked to the DNA markers on chromosome 14q. *Neurology* **44**, 1302–1308.
- Trotter, Y., Devys, D., Imbert, G., Saudou, F., An, I., Lutz, Y., Weber, C., Agid, Y., Hirsch, E.C., and Mandel, J.-L. (1995a). Cellular localization of the Huntington's disease protein and discrimination of the normal and mutated form. *Nature Genet.* **10**, 104–110.
- Trotter, Y., Lutz, Y., Stevanin, G., Imbert, G., Devys, D., Cancel, G., Saudou, F., Weber, C., David, G., Tora, L., et al. (1995b). Polyglutamine expansion as a pathological epitope in Huntington's disease and four dominant cerebellar ataxias. *Nature* **378**, 403–406.
- Wanker, E.E., Rovira, C., Scherzinger, E., Hasenbank, R., Walter, S., Tait, D., Collicelli, J., and Lehrach, H. (1997). HIP-1: A huntingtin interacting protein isolated by the yeast two hybrid system. *Hum. Mol. Genet.* **6**, 487–495.
- Weidenheim, K.M., and Dickson, D.W. (1995). Intranuclear inclusion bodies in an elderly demented woman: a form of intranuclear inclusion body disease. *Clin. Neuropathol.* **14**, 93–99.
- Yuasa, T., Ohama, E., Harayama, H., Yamada, M., Kawase, Y., Wakabayashi, M., Atsumi, T., and Miyatake, T. (1986). Joseph's disease: clinical and pathologic studies in a Japanese family. *Ann. Neurol.* **19**, 152–157.
- Zhuchenko, O., Bailey, J., Bonnen, P., Ashizawa, T., Stockton, D.W., Amos, C., Dobyns, W.B., Subramony, S.H., Zoghbi, H.Y., and Lee, C.C. (1997). Autosomal dominant cerebellar ataxia (SCA6) associated with small polyglutamine expansions in the alpha1A-voltage-dependent calcium channel. *Nature Genet.* **15**, 62–69.
- Zoghbi, H.Y. (1996). The expanding world of ataxins. *Nature Genet.* **14**, 237–238.